Open Access
Stechnolock: Biotechnology and Bioengineering
RESEARCH ARTICLE

Effect of Intratracheal Instillation of Zno Nanoparticles on Ovalbumin-Induced Allergic Asthma Mice

Mengying Xu[1,3*], Yanxia Liao[1,*], Lin Zhang[2], Juan Du[4], Ping Wang[2], Wen Zhao[5], Shuxian Yin[1], Hong Yang[1], XueXue[2], Yu Deng[2], Shaoxi Cai[1,&], Guodong Hu[1,&], Yinghua Chen[2,&]

[1]Department of Respiratory and Critical Care Medicine, Nanfang Hospital, Southern Medical University, Guangzhou 510515, Affiliated Dongguan Hospital, Southern Medical University, Dongguan, Guangdong 523059, China;

[2]Department of Histology and Embryology, Guangdong Provincial Key Laboratory of Construction and Detection in Tissue Engineering, NMPA Key Laboratory for Safety Evaluation of Cosmetics, School of Basic Medical Sciences, Southern Medical University, Guangzhou 510515, Dongguan People's Hospital Biobank, Affiliated Dongguan Hospital, Southern Medical University, Dongguan, Guangdong 523059, China;

[3]Department of Respiratory and Critical Care Medicine, the People's Hospital of Yangjiang, Yangjiang, 529500, China;

[4]Department of Inspection and Quarantine (Hygiene Detection Center), School of Public Health, Southern Medical University, Guangzhou, 510515, China;

[5]Department of Medical Imaging, Guangzhou Women and Children's Medical Center, National Children's Medical Center for South Central Region , Guangzhou 510515, China

* These authors contributed equally to this work and should be considered co-first authors

[*]Corresponding Author: Corresponding author: Yinghua Chen, Guangdong Provincial Key Laboratory of Construction and Detection in Tissue Engineering, Department of Histology and Embryology, School of Basic Medical Sciences, Southern Medical University, Guangzhou 510515, Dongguan People's Hospital Biobank, Affiliated Dongguan Hospital, Southern Medical University, Dongguan, Guangdong 523059, China. E-mail: mrchch@126.com; Guodong Hu, Department of Respiratory and Critical Care Medicine, Nanfang Hospital, Southern Medical University, Guangzhou 510515, Affiliated Dongguan Hospital, Southern Medical University, Dongguan, Guangdong 523059, China;. E-mail: huguodong@smu.edu.cn; Shaoxi Cai, Department of Respiratory and Critical Care Medicine, Nanfang Hospital, Southern Medical University, Guangzhou 510515, China;. E-mail: hxck@smu.edu.cn

Citation: Mengying Xu, Yanxia Liao, Lin Zhang, Juan Du, Ping Wang, et al. (2022) Effect of Intratracheal Instillation of Zno Nanoparticles on Ovalbumin-Induced Allergic Asthma Mice. Stechnolock: Biotech & Bioeng 1: 1-19

ABSTRACT

Asthma is a common chronic and repeated airway inflammatory disease that is an important health problem in most countries. Although studies have shown zinc oxide (ZnO) is one of predisposing factors of asthma, the adjuvant effects of ZnO on the advance of allergic asthma airway inflammation remains unclear. Here, the effects of nanoparticle-sized ZnO (nZnO) and bulk-sized ZnO (bZnO) on the ovalbumin (OVA)-induced asthma in mice were studied. Our results showed that exposure to nZnO in OVA-induced mice increased the levels of total protein, total cell number, neutrophil percentage and eosinophils in bronchoalveolar lavage fluid. Intratracheal instillation of nZnO intensively aggravated OVA-induced airway inflammation, alveolar exudation, accompanied by enhanced expression of Th2 cytokine. At the same time, nZnO could aggravate the production of reactive oxygen species (ROS) in the lung and cause airway damage. Also, cell apoptosis and DNA damage were more serious in asthma mice exposed to nZnO than in mice in other groups. This may be mediated via increased oxidative stress, which could lead to asthma-related cytokine expression, apoptosis and DNA damage. Moreover, this adjunct effect might active IL-33/ST2/ERK signaling to promote allergic asthma inflammation. These results suggest that nZno is not just a predisposing factor of ashma, individuals with allergic asthma exposed to nZnO might be more likely to make disease develop or exacerbate, especially in patients with asthma or occupational exposure to nZnO.

Keywords: Asthma; Zinc Oxide; Nanoparticles; Toxicity

Introduction

Asthma is a worldwide health problem that creates a great global burden. For example, it has a global prevalence ranging from 1 to 21% in adults (To et al., 2012). This chronic inflammatory disease of the airways is characterized by reversible airway obstruction, repeated airway inflammation, mucus hypersecretion, CD4+ T helper type 2 (Th2) lymphocytes, and airway hyperresponsiveness (Agrawal & Shao, 2010) [2]. The damaged mucosal barrier allows the body to be easily affected by a variety of occupational and environmental factors.

Nanotechnology is evident in many industrial manufacturing settings, such as energy, electronics, biomedical devices, paints, consumer products, and other fields (Landsiedel et al., 2010) [21]. Nanoparticle-sized zinc oxide (nZnO) is one of the major metal oxide nanoparticles. More than 300 companies around the world are producing in excess of 1.2 million tons of nZnO per year(Kumari et al., 2011) [19]. This increased production and application has also raised the likelihood for human exposure to nZnO at various steps of their synthesis (laboratory), manufacture (industry), use (i.e. consumer products, devices, and medicines), and disposal (Kumar et al., 2011). It has been reported that nanoparticles have a marked pulmonary toxicity compared with larger particles (Oberdörster, 2001; Wang et al., 2020) [31], and zinc is a crucial factor in lung inflammation among metals and metal oxide nanoparticles(Adamson et al., 2000) [1].

It was reported that several kinds of sicknesses can be expected from exposure to nZnO, including asthma, bronchitis, lung cancer, and others (Cho et al., 2011; Chuang et al., 2014; Weir et al., 1989) [7, 9, 44]. High ambient air coarse particulate matter (PM 2.5) zinc levels have been shown to be associated with increase pediatric asthma morbidity (Hirshon et al., 2008) [13]. Many animal studies indicate that nZnO induces allergic airway inflammation in mice. For example, infusing nZnO into mice increases the concentrations of eotaxin and interleukin-13 (IL-13) and IL-33 in the bronchoalveolar lavage fluid (BALF), and eosinophils were recruited to the alveolar interstitium (Cho et al., 2011). Also, nZnO particles can cause eosinophilic airway inflammation in mice without the allergens (K. L. Huang et al., 2015) [14]. The epidemiological and animal studies suggest that ZnO exposure might be related to asthma, but it is unclear whether inhaled exposure of nZnO to asthma patients will aggravate airway inflammation and cause more physical damage. Therefore, we investigated the roles of nZnO in asthma mouse model and compared these results with those induced by bulk-sized ZnO (bZnO) to better understand the influence of ZnO particle size on toxicity.

Materials and Methods

Nanoparticle characterization and preparation of suspensions

The bZnO and nZnO were purchased from Macklin (Shanghai, China) and Sigma-Aldrich (St. Louis, MO, USA), respectively. The morphology and size of the materials were characterized by transmission electron microscopy (TEM) (JEOL 2100F TEM, Jeol Ltd., Tokyo, Japan). The size of ZnO particles was measured by the Nano-ZS ZEN3600 (MALVERN Instr, Malvine, UK). Surface area of the powder composites was measured by a Micromeritics Instruments Corporation (ASAP 2020) BET (Brunauer, Emmett, and Teller) instrument using a nitrogen intrusion technique. The X-ray diffraction (XRD) pattern was recorded using a Rigaku Miniflex-II X-ray diffractometer (Tokyo, Japan). The ZnO particles were suspended in 2% sibling mouse serum in normal saline (NS). The suspensions were prepared by sonicating before oropharyngeal aerosolization.

Animals

Wild-type C57BL/6J mice aged 6-8 weeks (19-21 g) were obtained from Southern Medical University Experimental Animal Center. The mice were randomly divided into housing groups of four and housed in polypropylene cages with aspen chip bedding. The cages were stored in animal rooms with a 12-h light period from 8 a.m. to 8 p.m., temperature of 22 ± 2°, and relative humidity of 50 ± 5%. The cages were sanitized two times per week. All mice were given free access to tap water and standard diet. The animal studies in this report were performed according to the principles of the University of Southern Medical Animal Care Committee, which granted approval for these studies.

Ovalbumin (OVA)-induced allergic asthma mice

The mice were acclimated for 1 week and then sensitized. On days 1 and 7, the mice were injected intraperitoneally with 10 μg of OVA (Sigma) and 1 mg of $Al(OH)_3$ suspension. Then, the mice in the OVA group were challenged for 30 min per day with aerosolized 1% OVA in sterile water solution from day 8 to day 14. Control mice were sensitized and challenged with an equal volume of sterile water.

Experimental design and exposur

The mice were randomly divided into six groups: NS (vehicle control), bZnO, nZnO, OVA+NS, OVA+bZnO, and OVA+nZnO. The vehicle group received sterile water and NS. The bZnO group received sterile water and 18 μg of bZnO suspended in NS. The nZnO group received sterile water and 18 μg of nZnO suspended in NS. The OVA+NS group received an OVA challenge. The OVA+bZnO group included OVA-induced mice that received 18 μg of bZnO in NS. The OVA+nZnO group included OVA-induced mice that received 18 μg of nZnO in NS. The mice were administered ZnO solution or NS by oropharyngeal aerosolization on day 14. Animals were sacrificed 24 h after the ZnO challenge. The protocol is shown in Figure 1.

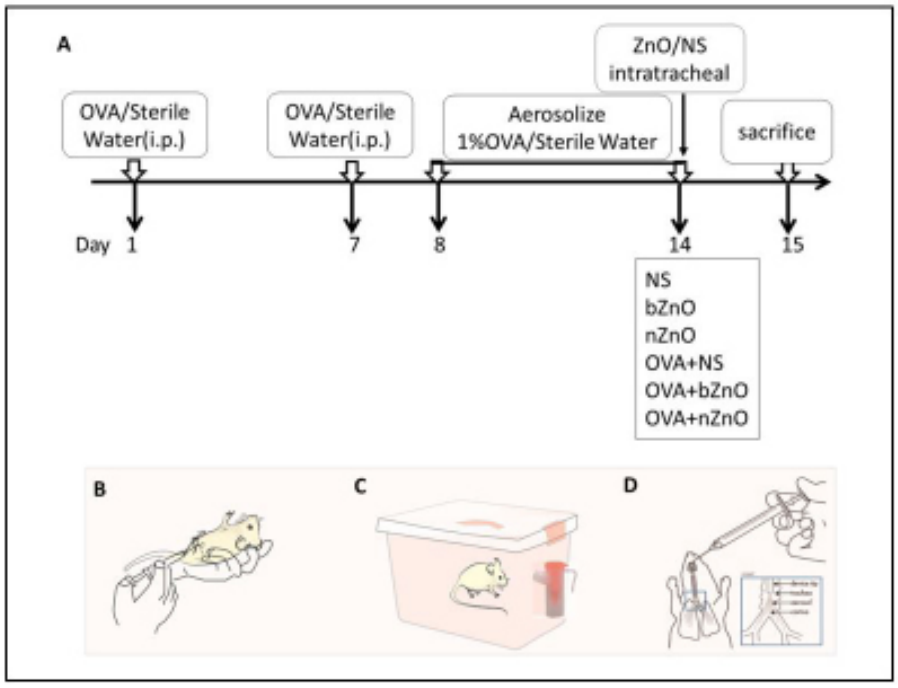

A: Study protocol. B: Intraperitoneal injection. C: Aerosolization. D: Intratracheal instillation. The mice were divided into the following six groups: NS, bZnO, nZnO, OVA+NS, OVA+bZnO, and OVA+nZnO. On days 1 and 7, mice were treated with 0.01% OVA/Al(OH)3 solution or sterile water for control by intraperitoneal injection. Then, on days 8 to 14, mice were challenged for 30 min per day with aerosolized 1% OVA or sterile water for controls. Both groups were exposed to 18 μg of bZnO or nZnO solution by oropharyngeal aerosolization under light anesthesia, compared to NS. Lastly, after 24 h of observation, all mice were sacrificed, and tissue samples (i.e. blood, BALF, lung, liver, and kidney) were collected.

Figure 1: Overview of the experimental design for ZnO exposure in asthma mice

Preparation of BALF and cell counting

Lung lobes were lavaged three times via cannulation of the trachea and flushing with 1 mL of 0.9% NaCl. The lavage fluid was centrifuged (200 g, 10 min, 4°C), and the cell-free supernatant was used for the measurement of protein content and quantification of selected cytokines. The cell pellet was used for enumeration of total and differential cell counts. The total cell count was determined on a fresh fluid specimen using a hemocytometer. The BALF cells were stained with Wright's-Giemsa Staining Solution (GBCBIO Technologies, Guangzhou, China), and the cellular composition was determined by scoring 200 cells.

Determination of total protein and inflammatory cytokines levels in BALF

The total protein concentration was quantified spectrophotometrically at 562 nm using a BCA Protein Assay Kit (GBCBIO). Luminex assays were performed according to the manufacturer's instructions (Luminex Corp., Austin, TX, USA) to determine the following cytokine levels: tumor necrosis factor (TNF-α), interleukin-1β (IL-1β), interleukin-4 (IL-4), interleukin-13 (IL-13), and interleukin-33 (IL-33). Enzyme-linked immunosorbent assays (ELISAs) were performed according to the manufacturer's instructions (Elabscience Biotech Co., Ltd., Wuhan, China) to determine macrophage chemoattractant protein-1 (MCP-1) and immunoglobulin E (IgE).

Histopathology and immunohistochemistry of lung tissues

The lung lobes were collected and fixed with 4% paraformaldehyde 48 h before being embedded in paraffin, sectioned at 5-μm thickness, and stained with hematoxylin & eosin (H&E) and Periodic Acid–Schiff (PAS) for identification of intraepithelial neutral and acidic mucosubstances in pulmonary bronchiolar epithelium. Immunohistochemical staining involved generation of serial paraffin sections for antigen retrieval. The sections were steamed for 20 min in followed by blocking of endogenous peroxidase (3% H2O2) and preincubation with serum. Primary antibodies against 8-hydroxy-2'-deoxyguanosine (8-OHdG; JalCA, Shizuoka, Japan), anti-F4/80 (eBioscience, San Diego, CA, USA), anti-pERK1/2 (Cell Signaling Technology, Danvers, MA, USA), anti-ST2 (abcam, Cambridge, MA) and anti-IL33 (abcam, Cambridge, MA) were used overnight at 4°C. DAB peroxidase substrate kit (Bios, Wuhan, China) was used to visualize the signals.

Measurement of oxidative stress parameter

Oxidative stress parameters were measured in the lung tissue homogenate. A portion of lung was homogenized with normal saline, and the preparation was centrifuged at 500g and 4°C for 10 min. The resultant supernatant was equilibrated with saline and used to determine the levels of protein in the tissue homogenates. The levels of catalase (CAT), glutathione (GSH), total superoxide dismutase (T-SOD), and malondialdehyde (MDA) were determined using commercial kits (Nanjing Jiancheng, Nanjing, China). The determinations were performed strictly according to the manufacturer's instructions.

Analyses of cell apoptosis

The left lobes of lung were taken out from 4% paraformaldehyde, embedded in paraffin for 24 h, and sectioned at 4-μm thickness. Sections treated for immunohistochemical staining were washed twice with phosphate-buffered saline and stained with Hoechst 33258 staining solution according to the manufacturer's instructions (Beyotime, Jiangsu, China).

Quantification of Zn^{2+} in different organs

The blood, lung, liver, spleen, kidney, heart and brain tissues from mice in each group were stored at −80°C immediately after resection. Tissues were lyophilized for 16 h and −50°C in a freeze dryer (Labconco Corp., Kansas City, MO, USA) and then weighed. The tissues were digested in a digestion system (XinHeda, Beijing, China) at 95-98°C using mixtures of high purity concentrated hydrochloric acid and nitric acid in 1:4 ratio, respectively. Metal analysis of the digested tissues was performed using inductively coupled plasma mass spectrometer (Xseries 2 quadrupole ICP-MS, Thermo Fisher Scientific Inc., West Palm Beach, FL, USA) with a method detection limit for Zn of less than 1 μg/kg. Each sample was spiked with cobalt as an internal standard at 20 μg/L.

Determination of serum biochemical parameters

The serum was obtained after centrifugation at 1200 g for 10 min. The biochemical indices were determined by an automatic biochemical analyzer (AU5800, BECKMAN COULTER, Tokyo, Japan) and included alanine aminotransferase (ALT), aspartate aminotransferase (AST), total protein (TP), alkaline phosphatase (ALP), urea (UREA), creatinine (CR), and creatine kinase (CK).

Statistical analysis

Statistical analyses were performed with SPSS 20.0 software. Data are expressed as means ± standard deviation. The independent samples T test or the Mann-Whitney U (nonparametric) test was performed to determine the difference between two samples. Comparisons of multiple samples were performed using the least significant difference (LSD) method in the presence of homogeneity of variance and Dunnett's T3 method in the presence of heterogeneity of variance. All statistical analyses were 2-tailed tests.

Results

Characterization of ZnO nanoparticle

The TEM images of bulk and nanoparticle agglomerates deposited on a TEM grid from a methanol solution are shown in Figure 2A and 2B. The diameters of individual particles, assessed by measurement of more than 200 particles, yielded primary particle size distributions of 147-375 nm and 24-60 nm for bZnO and nZnO particles, respectively. The XRD patterns for bZnO and nZnO particles are compared with that for standard crystalline zincite in Figure 2C and 2D. These data show that the particles have the same crystal structure as that of bulk zincite. The specific surface area of the sample was calculated, yielding a surface area of 3.342 m^2/g for the batch of bZnO and 19.418 m^2/g for the batch of nZnO used in the study. Dynamic light scattering showed that the particle size distributions of bZnO (Figure 2E) and nZnO (Figure 2F) in aqueous solution are approximately 958.9 and 195.3 nm, respectively, and that the zeta potentials of bZnO (Figure 2G) and nZnO (Figure 2H) are 34.5 and 45.7 mV, respectively. The results suggest that the nanoparticles are agglomerated in aqueous solution.

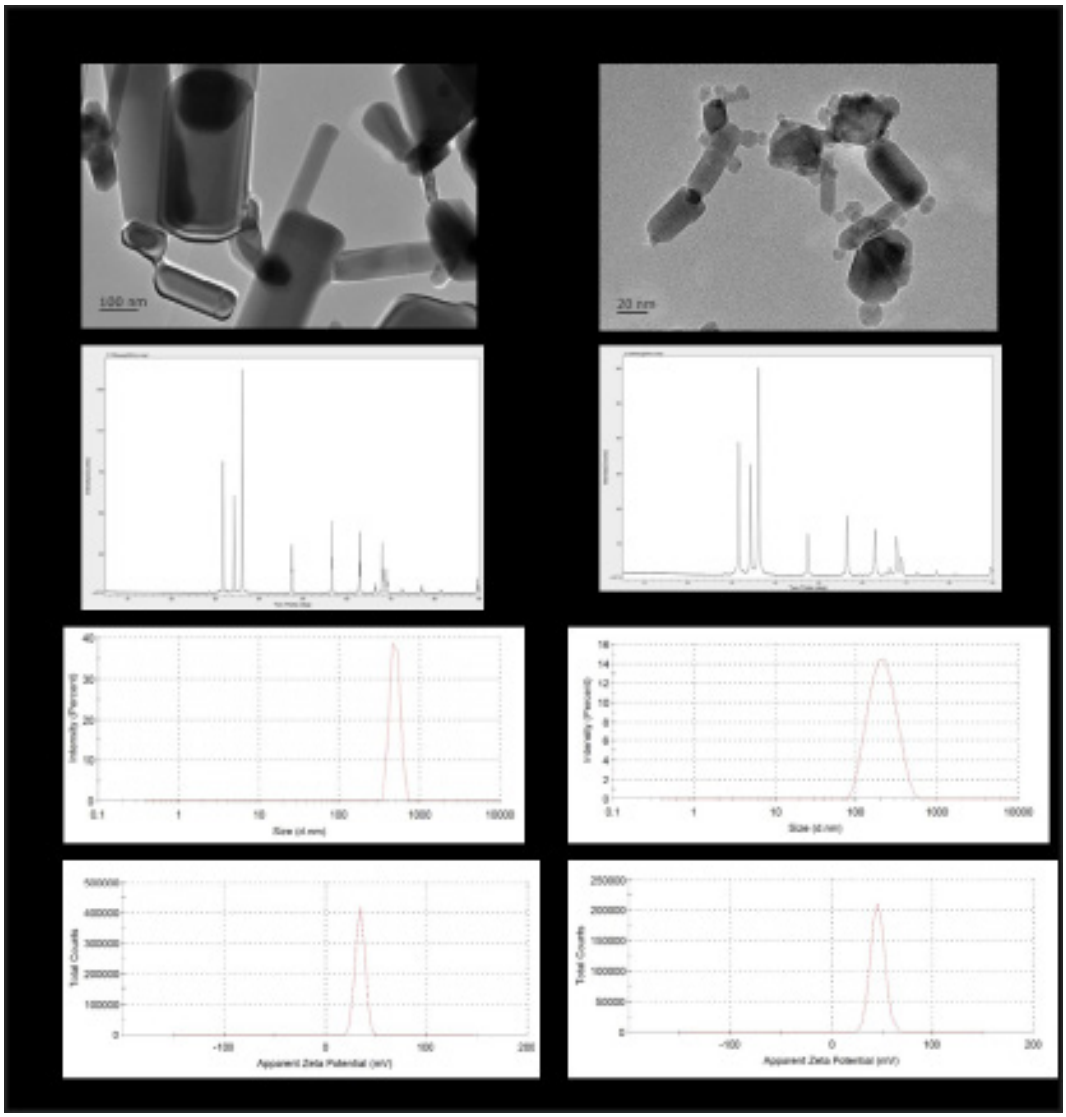

A,B: TEM images; C,D: The XRD spectrum patterns; E,F: Particle size distributions; G,H: Particle Zeta potential

Figure 2: Characterization of bulk and nano ZnO nanoparticles

Effects of ZnO particles on airway inflammation

The airway inflammation was determined by BALF analysis (Figure 3). The total number of cells was greater in the nZnO group compared to the bZnO group. The total number of cells was significantly greater in the OVA+nZnO group than in the OVA+bZnO and the OVA+NS groups (Figure 3A). We next analyzed the proportion of neutrophils in the BALF by Giemsa-Wright's staining (Figure 3B). The ZnO particles caused a greater proportion of neutrophils among total cells in the presence of OVA than in mice that were not challenged with OVA. The proportion was significantly greater in the OVA+nZnO group than in the OVA+bZnO, OVA+NS, and nZnO groups. The nZnO group had a greater eosinophil proportion than the bZnO group (Figure 3C). The OVA+nZnO group showed a higher eosinophils proportion than in the OVA+bZnO, OVA+NS, and the nZnO groups. Additionally, the concentration of proteins in BALF was elevated (Figure 3D). Mice treated with only nZnO had no difference in concentration of proteins in BALF compared with bZnO. In contrast, in the presence of OVA, the level was significantly higher in the OVA+nZnO group than the OVA+bZnO and the 0VA+NS groups.

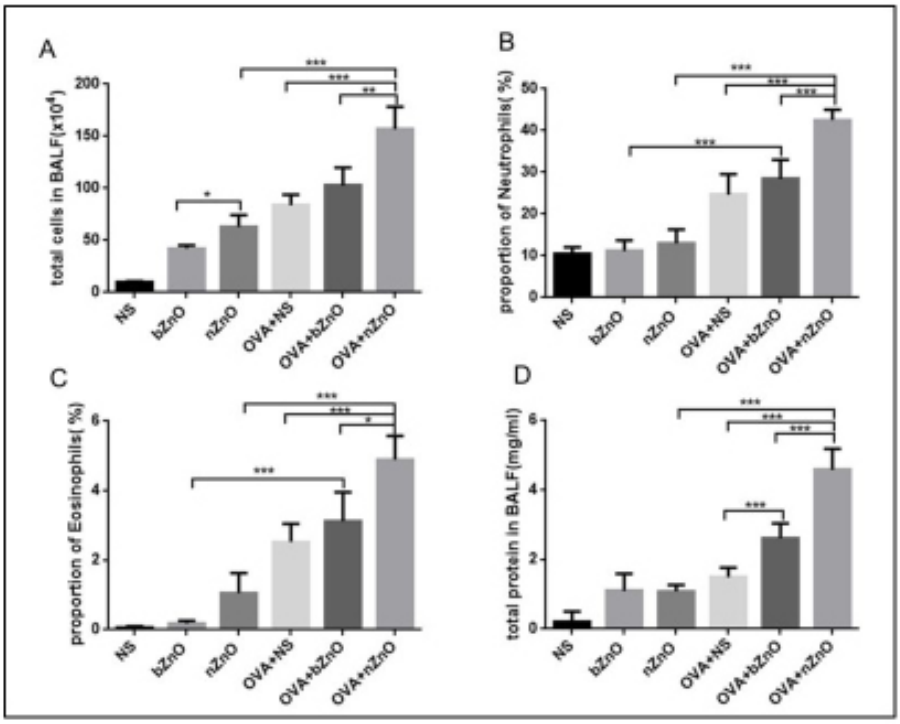

A: Total cell counts. B: The proportion of neutrophils among total cells. C: The proportion of eosinophils among total cells. D: Total protein. The data are presented as the mean ± SEM (n=6 for each treatment group). Key: (*) p<0.5, (**) p<0.01, (***) p<0.001.

Figure 3: Infiltration in the BALF of different group

Effects of ZnO particles on alveolar exudation by TEM method

Increasing effusion in pulmonary alveoli could reflect the development of allergic asthma(Agrawal & Shao, 2010). In our study, the dispersion of effusion and particles in alveoli and septum were observed by transitional electronic microscope (TEM) (Figure 4). There was no obvious exudation in the alveolar cavity in the NS group and the bZnO group. In the nZnO group, there was a little exudation in the alveolar cavity and scattered particles in the cells.

Compared with the OVA + NS group, alveolar exudation increased in the OVA + bZnO group. The OVA + nZnO group showed most obvious alveolar exudation and particle accumulation in cells—compared with all groups. In general, nZnO could promote particles penetration and alveolar exudation in OVA-induced asthma mice.

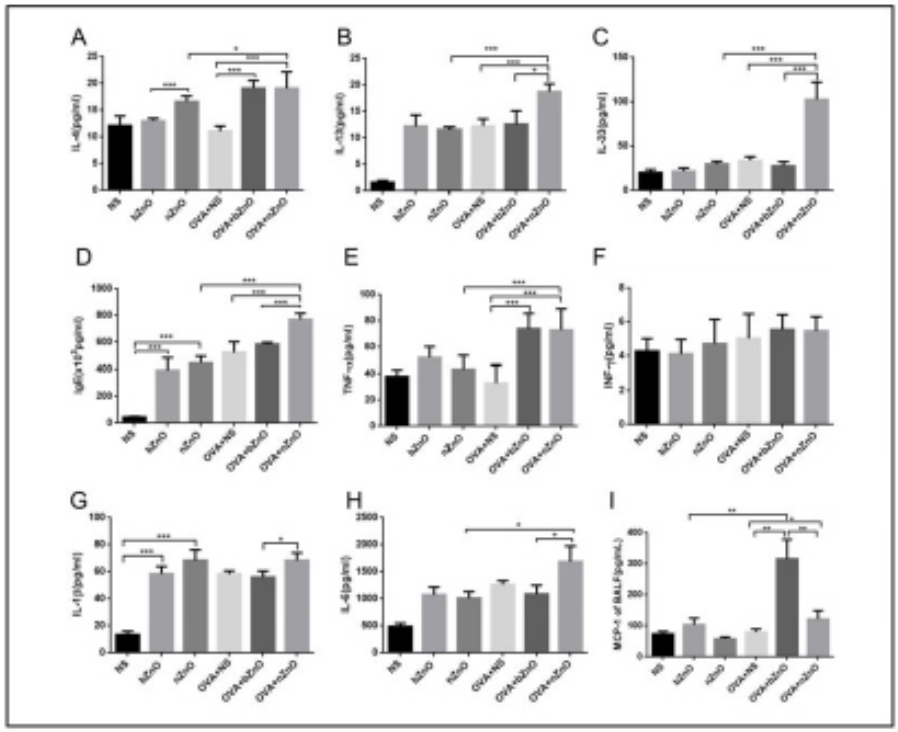

IL-4, IL-13, IL-33, IL-1β, TNF-a, INF-γ, and IL-6 in BALF were quantified by Luminex. IgE and MCP-1 in BALF were quantified by enzyme-linked immunosorbent assay. The data are presented as the mean ± SEM (n=6 for each treatment group). Key: (*) $p<0.05$, (**) $p<0.01$, (***) $p<0.001$

Figure 4: BALF cytokine levels of different groups

Effects of ZnO particles on the expression of cytokines in BALF

Inflammatory cytokines are one of the indicators to evaluate inflammation reaction. We measured protein levels of a series of cytokine released in the BALF after intratracheal instillation to investigate local cytokine released as it related to asthma (Figure 5). The level of IL-4 was higher in the nZnO group than in bZnO group. The OVA+nZnO group had greater IL-4 release than the nZnO group, and the level of IL-4 was higher in the OVA+nZnO and OVA+bZnO exposed groups than in the OVA+NS group. There was no statistical difference in the level of IL-4 between OVA+bZnO group and OVA+nZnO group. The level of IL-13 was highest in the OVA+nZnO group among the experimental groups. The level of IL-33 was almost 3-fold higher in the OVA+nZnO group than in the nZnO, OVA+NS, and OVA+bZnO groups. The level

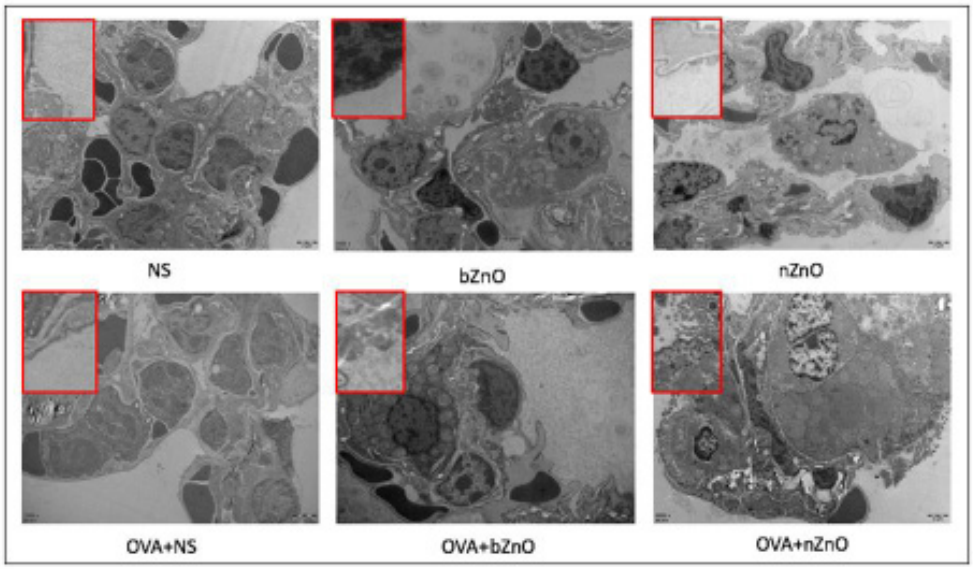

Lungs were sectioned and observed by transitional electronic microscope. The experimental groups are identical to NS, bZnO, nZnO, OVA+NS, OVA+bZnO, and OVA+nZnO.

Figure 5: SEM of lung

of IgE was higher in the nZnO and bZnO groups than the vehicle group, and there was no difference in IgE levels between the nZnO bZnO groups. In the presence of OVA, the OVA+nZnO group had higher IgE release than OVA+NS and OVA+bZnO groups.

The level of TNF-α was about 2-fold higher in the OVA+nZnO group than in the nZnO and OVA+NS groups. The differences in levels of IFN-γ did not reach statistical significance among groups. Compared to the NS group, the bZnO and nZnO group had higher IL-1β. There was no difference in the bZnO and nZnO group. In the presence of OVA, the level of IL-1β was higher in the nZnO-exposed group than that in the bZnO-exposed group. The level of IL-6 was higher in the OVA+nZnO group than the nZnO and OVA+bZnO groups. The level of MCP-1 in the OVA+nZnO group was slighter higher than that in the OVA+bZnO group. The level of MCP-1 was about 3-fold higher in the OVA+bZnO group than in the OVA+NS and OVA+nZnO groups.

Pathological characteristics of lung sections of mice

To determine the effects of ZnO particles on lung pathology, we evaluated lung tissue by H&E staining (Figure 6.1). Lung sections from NS and bZnO groups showed a normal bronchoalveolar structure with barely any inflammatory cell infiltration. The nZnO group showed a mild increase in inflammatory cells infiltrating the peribronchial and alveolar sections. In addition, the OVA+NS group showed bronchial cavity stenosis, bronchial epithelium shedding, mucin in the lumen, and some inflammatory cells around the airway. Compared to the OVA+NS group, the OVA+bZnO showed some epithelium cell shedding and an increase in prebronchial

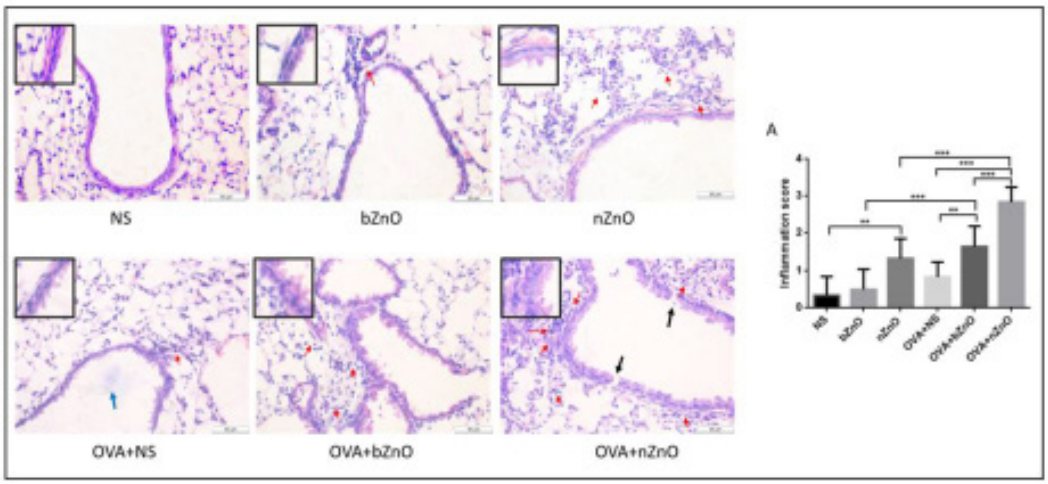

Figure 6.1: H&E staining of lung

inflammatory cells. The OVA+nZnO treatment showed the most serious damages, with partial bronchial wall rupture, basement membrane and smooth muscle layer significantly thickened, epithelial shedding, goblet cell proliferation, and infiltration of a large number of inflammation cells.

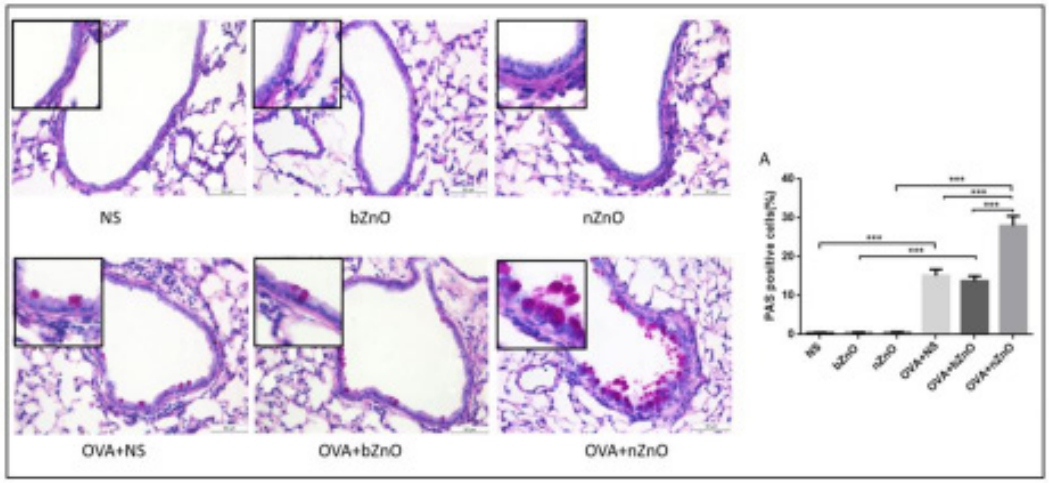

Figure 6.2: PAS staining of lung

We performed PAS-staining to further identify intraepithelial neutral and acidic mucosubstances in pulmonary bronchiolar epithelium (Figure 6.2). There was no positive change in mucosubstances in the vehicle group, bZnO group, or nZnO group. There was a slight increase in mucosubstances cells in the lungs from the OVA+NS group and the OVA+bZnO group. In contrast, OVA+nZnO markedly enhanced intraepithelial neutral and acidic mucosubstances in pulmonary bronchiolar epithelium.

Macrophages are important cells in organisms that remove particulate matter that are damaged when they perform defensive

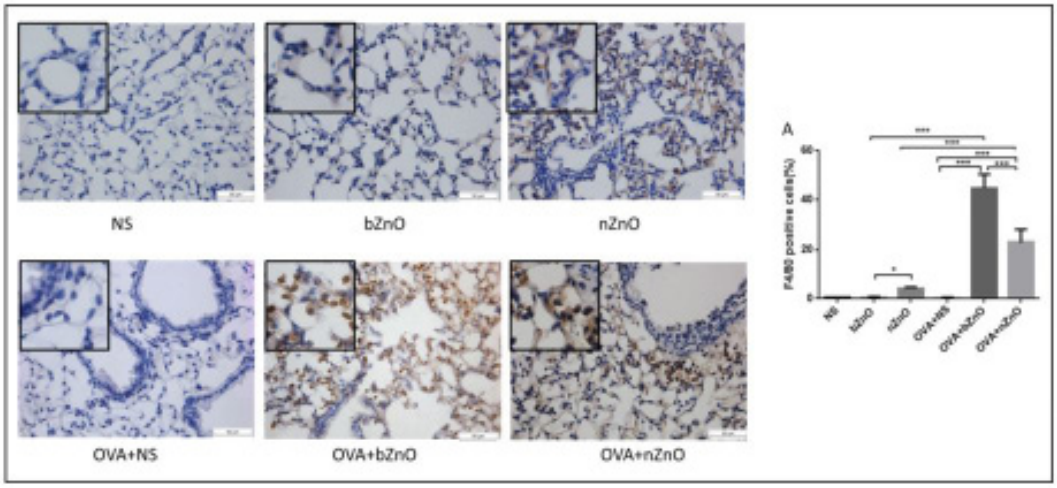

Figure 6.3: F4/80 staining of lung

Lungs were sectioned and stained with H&E, PAS, and F4/80. The experimental groups are identical to NS, bZnO, nZnO, OVA+NS, OVA+bZnO, and OVA+nZnO (red arrow: inflammatory cells; blue arrow: mucin in lumen; black arrow: bronchial wall rupture; Scar bars: 50 μm at 400× magnification). 5.1A: Inflammation score around bronchia in different groups. 5.2A: PAS positive cells (%). 5.3A: F4/80 positive cells (%). The data are presented as the mean ± SD (n=3 for each group). Key (*) p<0.5, (**) p<0.01, (***) p<0.001

Figure 6: Pathological characteristics of lung sections of mice

functions. Hence, we also performed F4/80 staining analysis to quantitate the positive cells among the experimental groups (Figure 6.3). The vehicle mice rarely showed a F4/80 positive cell. The number of cells stained with 4/80 in the lung of the nZnO group was slightly increased compared with bZnO group. The number of F4/80 positive cells was higher in the group challenged by OVA+bZnO and OVA+nZnO than that in the OVA+NS group. The OVA+bZnO group resulted in a greater number of F4/80 positive cells than

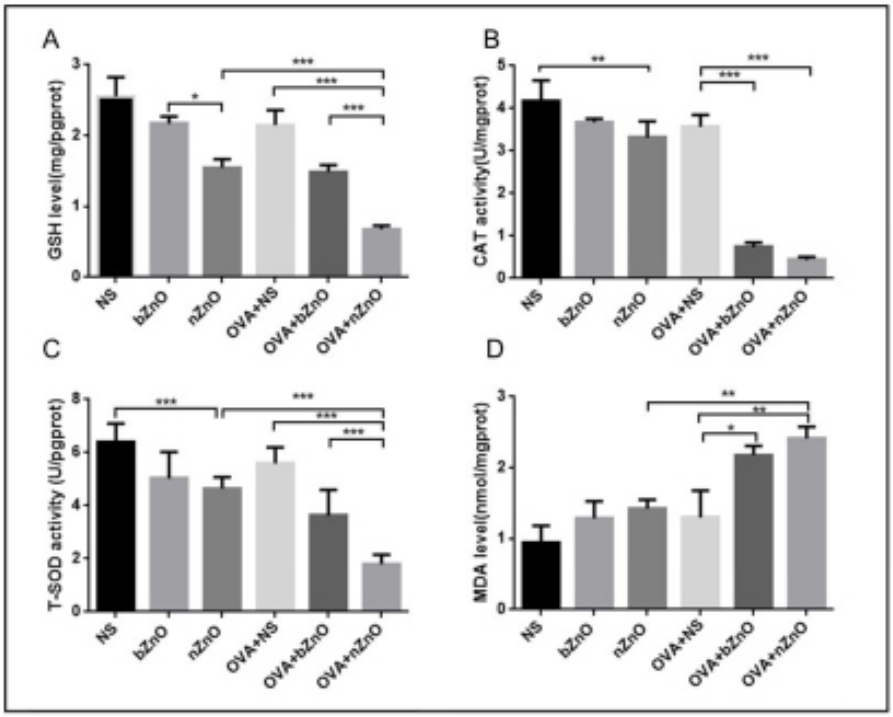

LA: GSH level (glutathione); B: CAT activity (catalase); C: T-SOD activity (total superoxide dismutase); D: MDA level (malondialdehyde). The data are presented as the mean ± SEM (n=6 for each treatment group). Key: (*) p<0.05, (**) p<0.01, (***) p<0.001.

Figure 7: Effects of ZnO exposure on oxidative stress in the lung

the bZnO group. Finally, the OVA+NS group had lower number of macrophages than did the OVA+bZnO group.

Measurement of the oxidative stress in lung

Oxidative stress kinase maintains a balance of intracellular redox reactions. To evaluate the aggravating effects of ZnO particles with oxidative damage, we determined the levels or activities of GSH, CAT, T-SOD, and MDA in lung tissue (Figure 7). Compared to the vehicle group, GSH level and CAT and T-SOD activities decreased in the nZnO group. The nZnO group had a lower GSH activity than the bZnO group

The results show that the T-SOD and CAT activities, and the GSH concentration in the lung were significantly decreased after nZnO challenged asthma model than other groups. Moreover, the OVA+nZnO group had lower GSH activities and T-SOD than OVA+bZnO particles. At the same time, the multiple ascending dose (MAD) concentration in the OVA+nZnO group was increased in only nZnO-challenged mice. The nZnO particles, but not the bZnO particles, promoted MDA production in the asthma model mice.

Evaluation of cells apoptosis in lung

Apoptosis reflects the toxic effect of particles to the lung. We characterized lung apoptosis in the lung by Hoechst 33258 staining after ZnO treatment (Figure 9). The OVA+nZnO group had the strongest positive cells among all experimental groups. The quantification of positive nuclei rate on Hoechst 33258 among the experimental groups is shown in Figure 9A. The proportion of positive nuclei in the nZnO group was higher than the bZnO group. The proportion in the OVA+nZnO group was greater than that in the OVA+NS group. In the presence of OVA, the proportion was increased in nZnO mice compared with bZnO mice.

Evaluation of DNA damage in lung

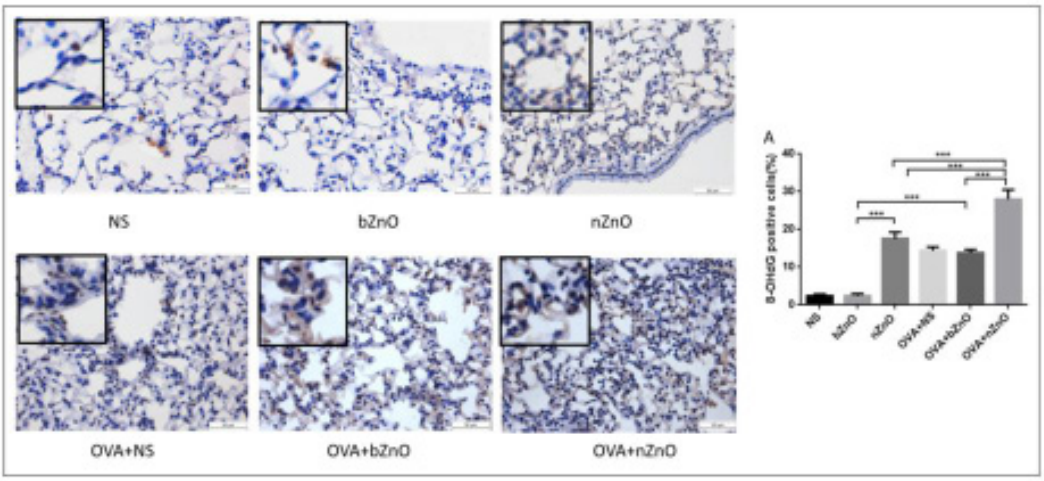

Lungs were sectioned and subjected to immunohistochemical staining with 8-hydroxyguanosine (8-OHdG, marker of DNA damage). The experimental groups are identical to NS, bZnO, nZnO, OVA+NS, OVA+bZnO, and OVA+nZnO (Scar bars: 50 μm at 400× magnification). Graph A shows the quantification of the area of positive staining presented as the mean ± standard deviation (n=3 mice per group). Key: (*) $p < 0.05$, (**) $p < 0.01$, (***) $p < 0.001$.

Figure 8: DNA damage in lung tissue after exposure to ZnO

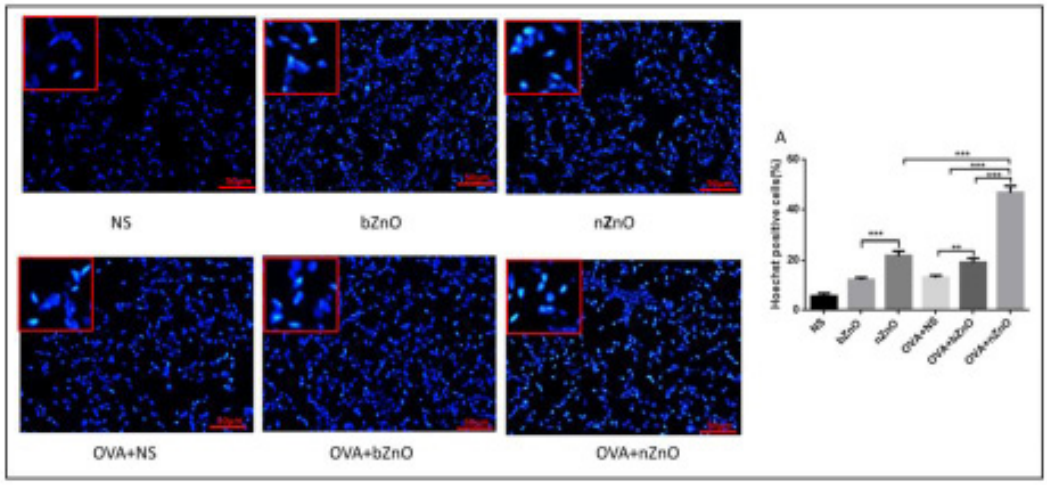

Hoechst33258 staining in the lung of the NS, bZnO, nZnO, OVA+NS, OVA+bZnO, and OVA+nZnO group. Scar bars: 50 μm at 400× magnification. Graph A shows the quantification of the area of positive staining presented as the mean ± standard deviation (n=3 mice per group). Key: (*) $p < 0.05$, (**) $p < 0.01$, (***) $p < 0.001$

Figure 9: Cells apoptosis in lung tissue after exposure to ZnO

To determine possible DNA damage, 8-OHdG was used (Figure 8). There was barely any positive staining for 8-OhdG in the NS and bZnO groups. The nZnO challenge induced moderate staining for 8-OhdG. There was no difference between the OVA+bZnO group and OVA+NS group. However, the OVA + nZnO group resulted in more severe 8-OHdG positive staining than the nZnO, OVA+NS, and OVA+bZnO groups. Results of analysis of the positive nuclei rate of 8-OHdG among the experimental groups are shown in Figure 8A. Compared with bZnO treatment, nZnO treatment resulted in an increased nuclei rate of 8-OHdG. The percentage of positive nuclei of 8-OHdG staining in OVA+nZnO group was greater than that in the nZnO group. In the presence of OVA, the

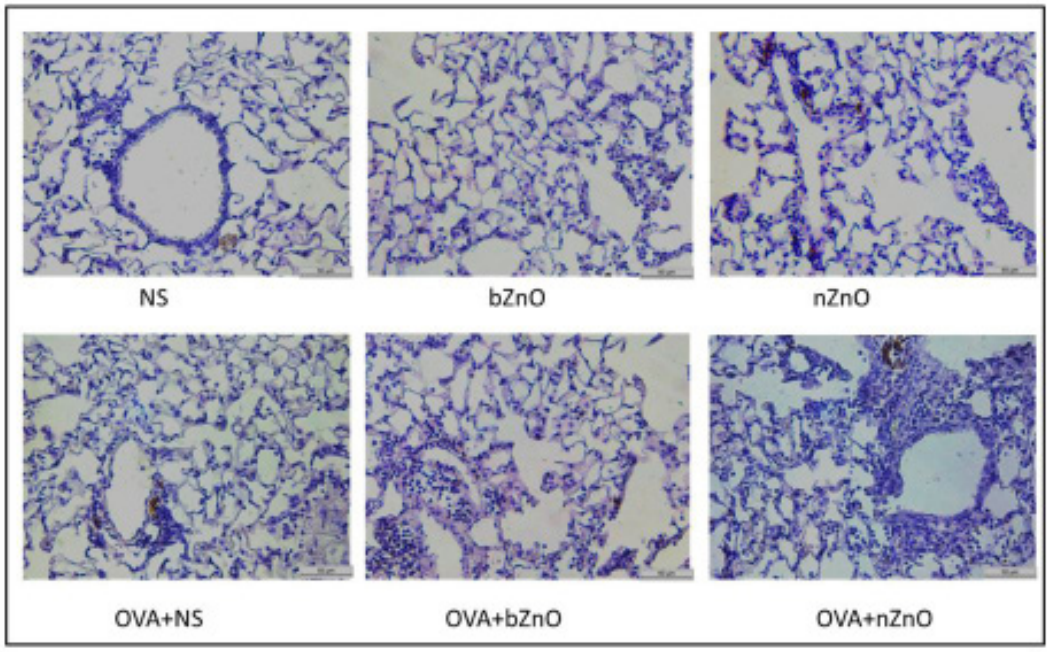

There are NS, bZnO, nZnO, OVA+NS, OVA+bZnO, and OVA+nZnO groups. Scar bars: 50 μm at 400× magnification

Figure 10.1: The expression of IL33 in lung tissue after ZnO exposed lung

positive cell rate was higher in the nZnO than the bZnO group.

Effects of ZnO particles on activation of IL-33/ST2/ERK signaling in lung tissue

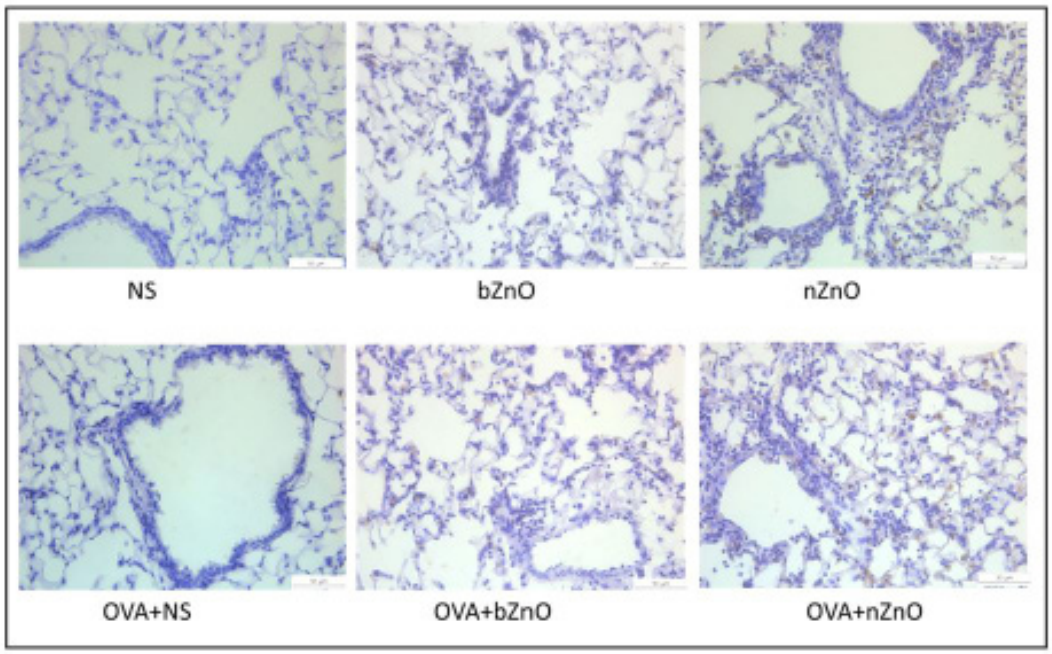

There are NS, bZnO, nZnO, OVA+NS, OVA+bZnO, and OVA+nZnO groups. Scar bars: 50 μm at 400× magnification

Figure 10.2: The expression of ST2 in lung tissue after ZnO exposed lung

Series of studies had suggested that IL-33 played an important role during the advance or exacerbation of asthma airway inflammation (Christianson et al., 2015; Gordon et al., 2016) [8, 12]. So we further performed immunohistochemistry staining to explore the probable signaling. The results (Figure.10.1) showed that nZnO markedly activated IL-33 in mice compared with the vehicle and bZnO groups. The OVA+nZnO group had the strongest expression of IL-33 among the experimental groups. In the presence of OVA, nZnO increased IL-33 secretion, compared with bZnO in lung.

The critical function of IL-33/ST2 (LI-33 receptor) signaling in allergic inflammation is illustrated by the fact that IL33 and IL1RL1

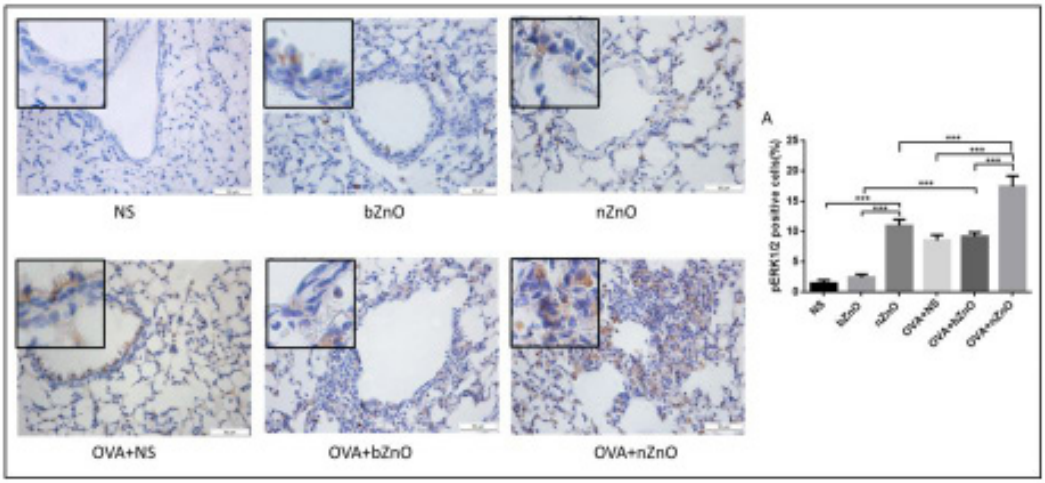

There are NS, bZnO, nZnO, OVA+NS, OVA+bZnO, and OVA+nZnO groups. Scar bars: 50 μm at 400× magnification. Graph A shows the quantification of the area of positive staining presented as the mean ± standard deviation (n=3 mice per group). Key: (*) $p < 0.05$, (**) $p < 0.01$, (***) $p < 0.001$

Figure 10.3: The expression of p-ERK1/2 in lung tissue after ZnO exposed lung

are among the most highly replicated susceptibility loci for asthma (Takatori et al., 2018) [39]. Consistent with IL-33 change in this study, the results (Figure. 10.2) showed that nZnO increased ST2 expression comparing to the vehicle and bZnO groups. The OVA-induce asthma mice had higher ST2 expression, especially after nZnO exposure.

IL-33 binds to heterodimeric receptor complex of ST2 and induces signalling through the extracellular-signal-regulated kinase (ERK) signaling pathway, which plays an important role in asthma inflammation (Drake & Kita, 2017; Liew et al., 2010) [11, 24]. Therefore, we detected the phosphorylation of ERK1/2 by immunohistochemical staining. The results showed that nZnO markedly activated ERK1/2 in mice compared with the vehicle and bZnO groups. There was no significant change in p-ERK1/2 between the bZnO group and the vehicle group. The OVA+nZnO group had the strongest expression of p-ERK1/2 among the experimental groups. In the presence of OVA, nZnO increased p-ERK1/2 expression in lung compared with bZnO. The quantification results are shown in Figure 10.3 A.

Discussion

It is well known that the increased prevalence of asthma in industrialized countries suggests that environmental derived cofactors are important in the development and persistence of asthma (Y. J. Huang, 2015) [15]. The first evidence for the potential role of zinc in asthma exacerbations comes from reports of zinc oxide exposure as a cause of occupational asthma in individuals working with heated zinc (Malo & Cartier, 1987) [27]. Nowadays, with the increasing production and use of nanometer materials like ZnO nanoparticles in many processes and human activities, people inevitably contact with ZnO during both production processing and postproduction. Therefore, inhalation of zinc oxide is potentially harmful to workers or others. In our study, we found that respiratory exposure to ZnO nanoparticles can aggravate allergic respiratory diseases, leading to more severe organ injury and pathological change caused by stronger oxidative stress.

Airway inflammation is considered to be a typical feature of allergic asthma (Murphy & O'Byrne, 2010) [29]. Usually the aggregation of eosinophils is a prominent feature of airway inflammation in ashma, and eosinophil-derived inflammatory mediators and cytokines lead to mucus hypersecretion and bronchoconstriction (Skevaki & Renz, 2018; Venturini et al., 2018) [37, 41]. Macrophages and neutrophils also play an important role in airway inflammation and participate in the process of tissue remodeling in allergic asthma (Lee and others 2004). In our study, the mice in the OVA + nZnO group had more serious airway destruction, more particle distribution and more inflammatory cell aggregates in the pulmonary and bronchial tissues after exposure to nZnO. The results showed that nZnO could further recruit eosinophils, macrophages, and neutrophils in the allergic asthma animal model. Although it is difficult to find eosinophils around the bronchus, cytokines in the BALF were easily detected 24 h after exposure. Furthermore, eosinophil-related cytokines were increased after nZnO treatment. In general, nZnO could promote and improve the inflammatory response and pathological changes in OVA-induced asthma mice.

Asthma is characterized by increase of Th2 immune respons and a series of chemokines (Barnes, 2001). Among these mediators, IL-4 plays an important role in the regulation of IgE production by B cells and is necessary for the optimal differentiation of Th2 cells. IL-13 has many functions similar to IL-4, and also regulates the production of IgE (Deo et al., 2010) [10]. In addition, it has been reported that IL-33 is an intrinsic cytokine of IL-1 family and is highly expressed in asthmatic patients (Préfontaine et al., 2009) [32]. Consistent with these findings, nZnO exposure in OVA-induced mice exacerbated the asthma response more than exposure to bZnO, such as increased neutrophils and eosinophils in BALF, and elevated levels of Th2 cytokines and chemokines (IL-4, IL-13, IL-33, and IL-6). Our research demonstrates that the exaggerated effect of nZnO on asthma inflammation related to OVA could be mediated through the enhanced expression of Th2 cytokines and chemokines (IL-4, IL-13, IL-33, and IL-6). Our results also indicate that nZnO increased OVA-induced inflammation more than bZnO.

We also studied the pro-inflammatory cytokines in BALF, including IL-1β, TNF-α, and MCP-1. These cytokines play an important role in the inflammation caused by the intratracheal instillation of particles (Cho and others 2007) [6] . In accordance with this, the expression levels of IL-1β, TNF-α, and IL-6 in asthma mice exposed to nZnO were significantly higher than those in asthma mice exposed bulk particles. Interestingly, in the asthma model, the concentration of MCP-1 caused by bulk particles was higher than that of nZnO. One possibility is that macrophages, the first barrier of cellular defense in the respiratory system, are also damaged when performing defense functions. As nZnO aggravated lung injury and the reactive of neutrophils gradually increased, MCP-1 may decrease, corresponding to the decrease of macrophage percentage. Collectively, our results demonstrate that nZnO exposure in asthma mice amplified inflammation compared with the bZnO group. Further research is needed to understand the mechanism behind these findings.

Oxidant-antioxidant imbalance also plays an important role in repeated cycles of airway inflammation in asthma (Al-Harbi et al., 2015) [3]. Imbalance or excessive production of oxidative stress and antioxidative capacity result in oxidative-related injury, which is usually represented by decreases in CAT, SOD, and GSH and an increase in MDA (Zhang et al., 2016) [46]. Our results show that T-SOD and CAT activities and GSH concentration in the lung were all significantly decreased in OVA-induced mice exposed to nZnO compared to control. These findings indicate that the exposure to nZnO could aggravate the production of reactive oxygen species (ROS) in the lung and cause airway injury. Therefore, we speculate that the defense system could not protect the asthma model effectively under oxidative stress.

Studies have demonstrated undesirable toxic effects of nZnO, such as inducing autophagic cell death, cell damage, and genotoxicity (Singh et al., 2009; Song et al., 2010; Wahab et al., 2014) [36, 38, 42]. Also, some studies have suggested that oxidative stress, cell apoptosis, and DNA damage were associated with the pathophysiology of asthma (Chan et al., 2016; Li et al., 2008; Mei et al., 2018) [5, 23, 28] . Our results showed that cell apoptosis and DNA damage were more serious in asthma mice exposed to nZnO than in mice in other groups. Collectively, the nZnO particles can promote allergic airway inflammation in asthma mice, which may be partly due to the increase of oxidative stress leading to the increase of DNA damage, apoptosis, and immune response.

Upon exposure to inhaled airborne allergens, lung cells secreted inflammatory cytokines that activated immune cells involved in type 2 immunity (Schmitz et al., 2005) [34]. Among various cytokines, interleukin (IL)-33 has been identified as having critical functions in the pathophysiology of allergic airway diseases Especially, IL-33/ST2 (IL-1RL1) axis has been regarded as the villain in allergic asthma Moreover, extracellular signal regulated protein kinases (ERK) signaling pathway plays an increasingly important role in airway inflammation and related to the severity of asthma and leads to cytokine production and degranulation (Jacob et al., 2002; Liu et al., 2008; Nel, 2002) [17, 25, 30] . And ERK pathway can be activated by IL-33/ST2 axis(Pushparaj et al., 2009) [33]. The activation of ERK is related to phospho-ERK mediated phosphatase activity, which is caused by Zn^{2+}-induced oxidant stress (Wu et al., 2013) [44]. To further explore the probable underlying mechanisms, we investigate the IL-33/ST2/ERK signaling expression. Our results showed that IL-33 expression increase in asthma mice exposed to nZnO than those in other groups. Correlated with IL-33, its receptor, ST2 increase in lung tissue after nZnO exposure than bZnO, especially on OVA-induced asthma mice. Moreover, nZnO markedly increased tyrosine phosphorylation of ERK1/2 without or with OVA presence. In conclusion, these findings indicated that IL-33/ ST2/ERK signaling pathway might play a potential role in the inflammatory response of nZnO in asthma model.

In addition, nanoparticles tend to migrate from pulmonary airways to other pulmonary compartments, such as epithelium/ endothelium, connective tissue, capillary lumen, or into systemic circulation (Oberdörster, 2001; Wang et al., 2020) [31, 43] . Under pre-existing pulmonary pathological conditions, the infiltration of Zn^{2+} into the blood may aggravate and cause high toxicity of nZnO (Inoue & Takano, 2011) [16]. In our study, the concentration of Zn^{2+} in blood, lung, liver, spleen and brain of nZnO group was significantly higher than that of bZnO group (Figure s1). After asthma mice exposed with nZnO, an increasing level of these enzymes (AST, ALT, CR and UREA) were observed in serum, which were related to the injury of hepatocyte cells and kidney tissue (Figure s3). The above results suggested that in the asthma model, the damage of some organs caused by nZnO was more serious than that caused by bulk particles.

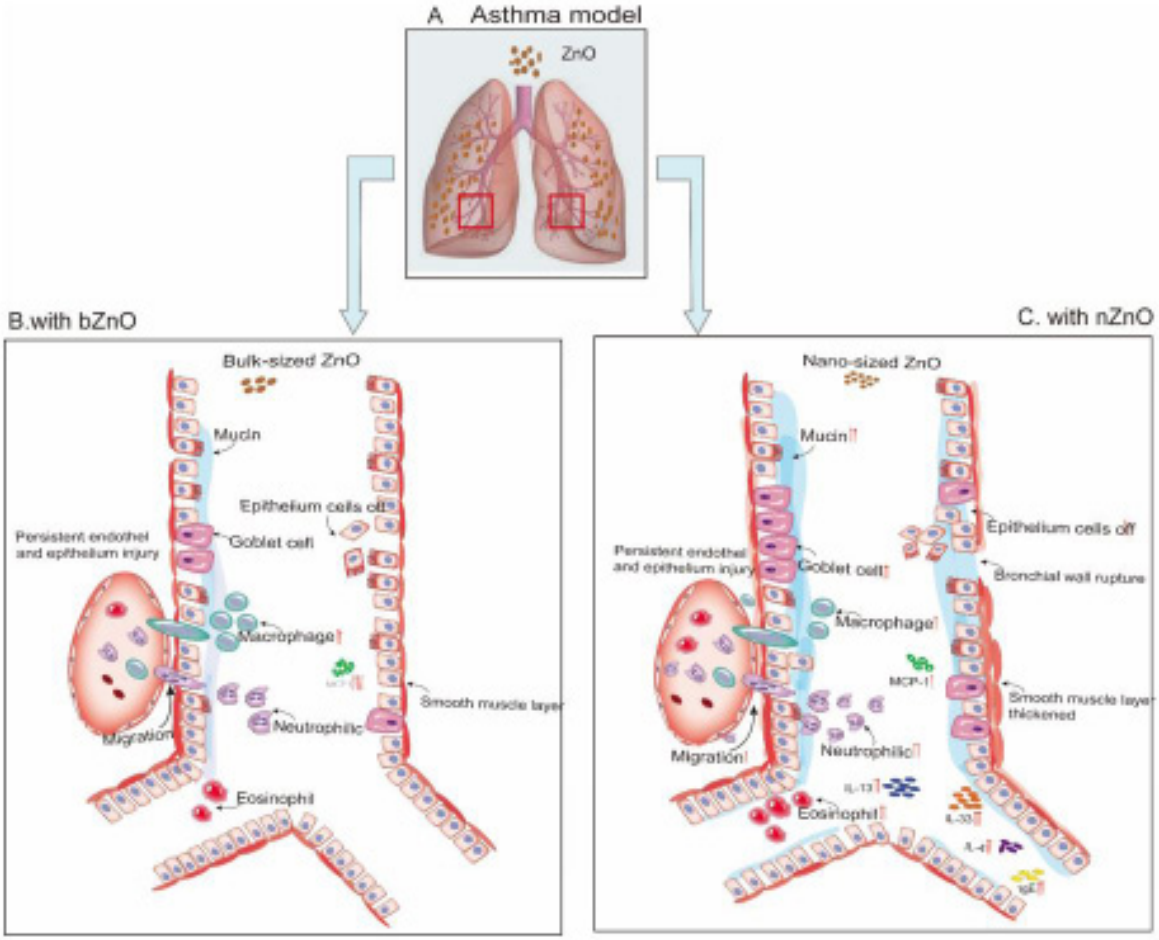

A schematic illustration of impact of bZnO and nZnO on OVA-induced allergic airway. In this study, we identified bZnO-enhanced airway inflammation was mediated by the increased macrophages and expression of MCP-1. However, nZnO-enhanced lung inflammation was mainly mediated by the increased neutrophils, eosinophils and expression of IL-33 ,IL-13, IgE and IL-4.

Figure 11: Schematic illustration of airway inflammation on asthma model after ZnO exposure

In conclusion, these results suggested that nZnO enhanced allergic inflammation related to asthma was mediated by increasing Th2 immune responses. Therefore, we proposed that individuals exposed to nZnO may be more likely develop or exacerbate allergic asthma by ROS and resulted in lung apoptosis and DNA damage. We also found that nZnO could permeate into the damaged airway epithelial barrier and then entered other organs by circulating blood, and even caused organ dysfunction. These results reveal a new aspect of nZnO toxicity, which has particular relevance to occupational nanoparticle exposure. The role of bZnO and nZnO in the OVA-induced asthma mice is summarized in Figure 11.

Acknowledgements

Special thanks to the guidance of professor Longquan Shao and the members of his group. This project was supported by the following grants: the Natural Science Funding of Guangdong Province (2022A1515012312, 2021A1515010023), the National Natural Science Funding of China (82070083), and Guangzhou Science and Technology Planning Project (20190203002), and Science and Technology Planning Project of Yangjiang City(SF2021064).

Declaration of Conflicting Interests

The author/authors declared no potential conflicts of interest with respect to the research, authorship, and/or publication of this article.

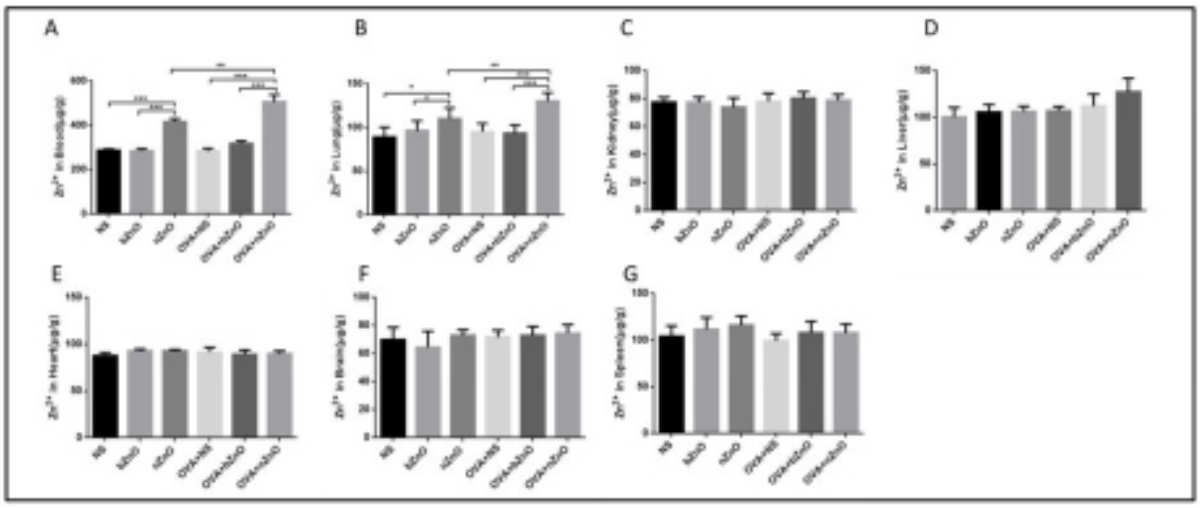

The amount of ZnO in different organs was quantified and shown in ZnO mass (mg) per gram dry tissue representing the ZnO mass density in each organ (n=6 for each group). The organs were collected 24 h after second treatment. Panels A, B, C, D, E, F, and G represent ZnO distribution in blood, lung, liver, brain, kidney, spleen, and heart, respectively. Key: (*) p<0.05, (**) p<0.01, (***) p<0.01

Figure S1: Zn^{2+} Concentration in organs of different group mice determined by ICP-MS

Group	Weight (X±S, g, n=6)
NS	0.030±0.009
bZnO	1.077±0.240[A]
nZnO	1.267±0.308[A]
OVA+NS	0.110±0.372
OVA+bZnO	1.417±0.372[B]
OVA+nZnO	2.503±0.428 [B,C,D]

The data are presented as the mean ± SD (n=6 for each group). Key: [A]p<0.001, compared to the NS group; [B]p<0.001, compared to the OVA+NS group; [C]p<0.001, compared to the nZnO group; [D]p<0.05, compared to the OVA+bZnO group

Figure S2: Body weight-loss of mice in different groups

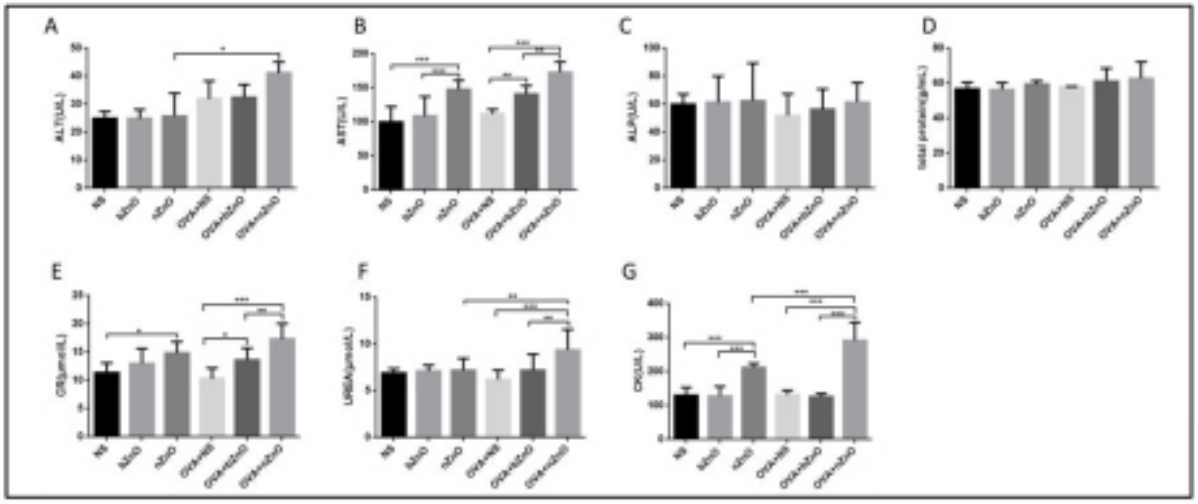

A: aspartate aminotransferase (AST), B: alanine aminotransferase (ALT), C: ALT/AST, D: alkaline phosphatase (ALP), E: total protein, F: lactate dehydrogenase (LDH), G: creatinine (CR), H: urea (UREA), I: creatine kinase (CK). Key: (**) p<0.01; (*) p<0.05

Figure S3: Alteration in serum biochemical parameters in different groups

References

1. Adamson IY, Prieditis H, Hedgecock C, Vincent R (2000) Zinc is the toxic factor in the lung response to an atmospheric particulate sample. Toxicol Appl Pharmacol 166: 111-9.

2. Agrawal DK, Shao Z (2010) Pathogenesis of allergic airway inflammation. Curr Allergy Asthma Rep 10: 39-48.

3. Al-Harbi NO, Nadeem A, Al-Harbi MM, Imam F, Al-Shabanah OA (2015) Oxidative airway inflammation leads to systemic and vascular oxidative stress in a murine model of allergic asthma. Int Immunopharmacol 26: 237-45.

4. Barnes PJ (2001) Th2 cytokines and asthma: an introduction. Respir Res 2: 64-5.

5. Chan TK, Loh XY, Peh HY, Tan W, Tan W (2016) House dust mite-induced asthma causes oxidative damage and DNA double-strand breaks in the lungs. J Allergy Clin Immunol 138: 84-96.e1.

6. Cho WS, Choi M, Han BS, Cho M, Oh J (2007) Inflammatory mediators induced by intratracheal instillation of ultrafine amorphous silica particles. Toxicol Lett 175: 24-33.

7. Cho WS, Duffin R, Howie SE, Scotton CJ, Wallace WA (2011) Progressive severe lung injury by zinc oxide nanoparticles; the role of Zn2+ dissolution inside lysosomes. Part Fibre Toxicol 8:27.

8. Christianson CA, Goplen NP, Zafar I, Irvin C, Good JJ, et al. (2015) Persistence of asthma requires multiple feedback circuits involving type 2 innate lymphoid cells and IL-33. J Allergy Clin Immunol 136: 59-68e14.

9. Chuang HC, Juan HT, Chang CN, Yan YH, Yuan TH, et al. (2014) Cardiopulmonary toxicity of pulmonary exposure to occupationally relevant zinc oxide nanoparticles. Nanotoxicology 8: 593-604.

10. Deo SS, Mistry KJ, Kakade AM, Niphadkar PV (2010) Role played by Th2 type cytokines in IgE mediated allergy and asthma. Lung India 27: 66-71.

11. Drake LY, Kita H. 2017. IL-33: biological properties, functions, and roles in airway disease. Immunol Rev 278(1):173-184.

12. Gordon ED, Simpson LJ, Rios CL, Ringel L, Lachowicz-Scroggins ME, et al. (2016) Alternative splicing of interleukin-33 and type 2 inflammation in asthma. Proc Natl Acad Sci USA 113: 8765-70.

13. Hirshon JM, Shardell M, Alles S, Powell JL, Squibb K, et al. (2008) Elevated ambient air zinc increases pediatric asthma morbidity. Environ Health Perspect 116: 826-31.

14. Huang KL, Lee YH, Chen HI, Liao HS, Chiang BL, et al. (2015) Zinc oxide nanoparticles induce eosinophilic airway inflammation in mice. J Hazard Mater 297: 304-12.

15. Huang YJ (2015) The respiratory microbiome and innate immunity in asthma. Curr Opin Pulm Med 21: 27-32.

16. Inoue K, Takano H (2011) Aggravating impact of nanoparticles on immune-mediated pulmonary inflammation. Scientific World Journal 11: 382-90.

17. Jacob A, Cooney D, Pradhan M, Coggeshall KM (2002) Convergence of signaling pathways on the activation of ERK in B cells. J Biol Chem 277: 23420-6.

18. Kumar A, Dhawan A, Shanker R (2011) The need for novel approaches in ecotoxicity of engineered nanomaterials. J Biomed Nanotechnol 7: 79-80.

19. Kumari M, Khan SS, Pakrashi S, Mukherjee A, Chandrasekaran N (2011) Cytogenetic and genotoxic effects of zinc oxide nanoparticles on root cells of Allium cepa. J Hazard Mater 190: 613-21.

20. Kurowska-Stolarska M, Stolarski B, Kewin P, Murphy G, Corrigan CJ, et al. (2009) IL-33 amplifies the polarization of alternatively activated macrophages that contribute to airway inflammation. J Immunol 183: 6469-77.

21. Landsiedel R, Ma-Hock L, Kroll A, Hahn D, Schnekenburger J (2010) Testing metal-oxide nanomaterials for human safety. Adv Mater 22: 2601-27.

22. Lee CC, Liao JW, Kang JJ (2004) Motorcycle exhaust particles induce airway inflammation and airway hyperresponsiveness in BALB/C mice. Toxicol Sci 79: 326-34.

23. Li N, Xia T, Nel AE (2008) The role of oxidative stress in ambient particulate matter-induced lung diseases and its implications in the toxicity of engineered nanoparticles. Free Radic Biol Med 44: 1689-99.

24. Liew FY, Pitman NI, McInnes IB (2010) Disease-associated functions of IL-33: the new kid in the IL-1 family. Nat Rev Immunol 10: 103-10.

25. Liu W, Liang Q, Balzar S, Wenzel S, Gorska M, et al. (2008) Cell-specific activation profile of extracellular signal-regulated kinase 1/2, Jun N-terminal kinase, and p38 mitogen-activated protein kinases in asthmatic airways. J Allergy Clin Immunol 121: 893-902.e2.

26. Magat JM, Thomas JL, Dumouchel JP, Murray F, Li WX, et al. (2020) Endogenous IL-33 and Its Autoamplification of IL-33/ST2 Pathway Play an Important Role in Asthma. J Immunol 204: 1592-1597.

27. Malo JL, Cartier A (1987) Occupational asthma due to fumes of galvanized metal. Chest 92: 375-7.

28. Mei M, Song H, Chen L, Hu B, Bai R (2018) Early-life exposure to three size-fractionated ultrafine and fine atmospheric particulates in Beijing exacerbates asthma development in mature mice. Part Fibre Toxicol 15: 13.

29. Murphy DM, O'Byrne PM (2010) Recent advances in the pathophysiology of asthma. Chest 137: 1417-26.

30. Nel AE (2002) T-cell activation through the antigen receptor. Part 1: signaling components, signaling pathways, and signal integration at the T-cell antigen receptor synapse. J Allergy Clin Immunol 109: 758-70.

31. Oberdörster G (2001) Pulmonary effects of inhaled ultrafine particles. Int Arch Occup Environ Health 74: 1-8.

32. Préfontaine D, Lajoie-Kadoch S, Foley S, Audusseau S, Olivenstein R, et al. (2009) Increased expression of IL-33 in severe asthma: evidence of expression by airway smooth muscle cells. J Immunol 183: 5094-103.

33. Pushparaj PN, Tay HK, H'Ng SC, Pitman N, Xu D, et al. (2009) The cytokine interleukin-33 mediates anaphylactic shock. Proc Natl Acad Sci USA 106: 9773-8.

34. Schmitz J, Owyang A, Oldham E, Song Y, Murphy E, et al. (2005a) IL-33, an interleukin-1-like cytokine that signals via the IL-1 receptor-related protein ST2 and induces T helper type 2-associated cytokines. Immunity 23: 479-90.

35. Schmitz J, Owyang A, Oldham E, Song Y, Murphy E, et al. (2005b) IL-33, an interleukin-1-like cytokine that signals via the IL-1 receptor-related protein ST2 and induces T helper type 2-associated cytokines. Immunity 23: 479-90.

36. Singh N, Manshian B, Jenkins GJ, Griffiths SM, Williams PM, et al. (2009) Nano Genotoxicology: the DNA damaging potential of engineered nanomaterials. Biomaterials 30: 3891-914.

37. Skevaki C, Renz H (2018) Advances in mechanisms of allergic disease in 2017. J Allergy Clin Immunol 142: 1730-1739.

38. Song W, Zhang J, Guo J, Zhang J, Ding F (2010) Role of the dissolved zinc ion and reactive oxygen species in cytotoxicity of ZnO nanoparticles. Toxicol Lett 199: 389-97.

39. Takatori H, Makita S, Ito T, Matsuki A, Nakajima H (2018) Regulatory Mechanisms of IL-33-ST2-Mediated Allergic Inflammation. Front Immunol 9: 2004.

40. To T, Stanojevic S, Moores G, Gershon AS, Bateman ED, et al. (2012) Global asthma prevalence in adults: findings from the cross-sectional world health survey. BMC Public Health 12: 204.

41. Venturini CL, Macho A, Arunachalam K, de Almeida D, Rosa S, et al. (2018). Vitexin inhibits inflammation in murine ovalbumin-induced allergic asthma. Biomed Pharmacother 97: 143-151.

42. Wahab R, Siddiqui MA, Saquib Q, Dwivedi S, Ahmad J, et al. (2014) ZnO nanoparticles induced oxidative stress and apoptosis in HepG2 and MCF-7 cancer cells and their antibacterial activity. Colloids Surf B Biointerfaces 117: 267-76.

43. Wang P, Zhang L, Liao Y, Du J, Xu M, et al. (2020) Effect of Intratracheal Instillation of ZnO Nanoparticles on Acute Lung Inflammation Induced by Lipopolysaccharides in Mice. Toxicol Sci 173: 373-386.

44. Weir DC, Robertson AS, Jones S, Burge PS (1989) Occupational asthma due to soft corrosive soldering fluxes containing zinc chloride and ammonium chloride. Thorax 44: 220-3.

45. Wu W, Bromberg PA, Samet JM (2013) Zinc ions as effectors of environmental oxidative lung injury. Free Radic Biol Med 65: 57-69.

46. Zhang HX, Liu SJ, Tang XL, Duan GL, Ni X, et al. (2016) H2S Attenuates LPS-Induced Acute Lung Injury by Reducing Oxidative/Nitrative Stress and Inflammation. Cell Physiol Biochem 40: 1603-1612.